Journal of the European Ceramic Society 37 (2017) 1059–1065

Contents lists available at www.sciencedirect.com

Journal of the European Ceramic Society

journal homepage: www.elsevier.com/locate/jeurceramsoc

Feature article

# Densification and grain growth of $Gd_2Zr_2O_7$ nanoceramics during pressureless sintering

Mao Zhou[a,b], Zhangyi Huang[a,b], Jianqi Qi[a,b,*], Nian Wei[a,c], Di Wu[d], Qinghua Zhang[a,b], Shanshan Wang[a,b], Zhao Feng[a,b], Tiecheng Lu[a,b,c,*]

[a] College of Physical Science and Technology, Sichuan University, Chengdu 610064, China
[b] Key Laboratory of Radiation Physics and Technology of Ministry of Education, Sichuan University, Chengdu 610064, China
[c] Key Laboratory of High Energy Density Physics of Ministry of Education, Sichuan University, Chengdu 610064, China
[d] The Gene and Linda Voiland School of Chemical Engineering and Bioengineering, Washington State University, Pullman, WA 99163, United States

ARTICLE INFO

*Article history:*
Received 16 July 2016
Received in revised form
19 September 2016
Accepted 19 September 2016
Available online 4 October 2016

*Keywords:*
$Gd_2Zr_2O_7$ nanoceramics
Pressureless method
Densification behavior
Two-step sintering

ABSTRACT

$Gd_2Zr_2O_7$ nanoceramics were fabricated using pressureless sintering method, in which the nanopowders were synthesized via solvothermal approach. The effects of starting powders on grain growth and densification during sintering of ceramics were revealed. Two distinct pressureless sintering methods were investigated, including conventional and two-step sintering. The sample grain size increases abruptly as sintering temperature increases during conventional sintering. In contrast, in two-step sintering, abnormal or discontinuous grain growth was suppressed in the second step, leading to $Gd_2Zr_2O_7$ nanoceramics formation (average grain size 83 nm, relative density ~93%). Such distinct behaviors may originate from the interplay between kinetic factors such as grain boundary migration and diffusion. Moreover, suppression of grain growth and promotion of densification in the two-step sintering are mainly due to dominant role of grain boundary diffusion during the second-step sintering process.



## 1. Introduction

Substantial efforts have been made to design and optimize sintering strategies to achieve accurately controlled grain growth and densification in fabrication of nanoceramics [1]. Nanoceramics have many advantages, such as low energy, minimized residual porosity and reduced crystallographic thermal expansion owing to decreased firing temperature [2].

Typically, the nanoparticles in ceramics have high surface energy, which may alter its structure and morphology, for example, stabilizing a metastable phase [3]. However, fabrication of dense bulk nanocrystalline ceramics is very challenging, since to make high-density ceramics high sintering temperature is necessary, which usually leads to inevitable grain coarsening. In contrast, sintering at lower temperature can only produce materials with smaller grain size. High-density is usually sacrificed [4]. Moreover, the sintered density is very sensitive to even slight sintering temperature variation [5]. At high temperature, single grain can grow rapidly by consuming a large numbers of surrounding grains, in which smaller grains dissolve and feed crystal growth of larger particles [6,7]. Notably, closed pores are mostly isolated from grain boundaries as a result of discontinuous grain growth [8]. Fine grain size and full densification are two competing factors of the most importance for nanoceramic fabrication [9].

Owing to its promising applications for nuclear waste disposal and thermophysical properties, numerous studies have been performed on $Gd_2Zr_2O_7$ [10,11]. Although it has potential to be employed as thermal barrier coating material, the relatively poor fracturing toughness limits its application [12]. Ceramics with nano-sized grains can overcome these drawbacks [13]. Sintering methods such as spark plasma and microwave sintering [14–16] were employed to sinter $Gd_2Zr_2O_7$ nanoceramics with improved properties. Xu et al. [16] obtained ceramics with a 92% final density and a grain size of 20 μm using microwave sintering of $Gd_2Zr_2O_7$ compacts, while abnormal grain growth were observed. However, spark plasma sintering has several intrinsic disadvantages. First, it is difficult to analyze the diffusion mechanism and trace the exact sintering process. In addition, this technique also requires expensive equipment setup, which is not cost effective [1].

Using microwave sintering, Lu et al. sintered ceramics with small grain size (2.4 μm) and high density [17]. Nevertheless, it was difficult to monitor and control sintering temperature in

* Corresponding authors at: College of Physical Science and Technology, Sichuan University, Chengdu 610064, China.
*E-mail addresses:* qijianqi@scu.edu.cn, qijianqi@gmail.com (J. Qi), lutiecheng@scu.edu.cn (T. Lu).

http://dx.doi.org/10.1016/j.jeurceramsoc.2016.09.019
0955-2219/

**Table 1**
Conditions of preparing green pellets.

| Samples | Calcination temperature of starting powders (°C) | Pressure (MPa) | ρ (g/cm$^3$) | ρ (%) |
|---|---|---|---|---|
| 1 | 800 | 10 | 3.59 ± 0.13 | 52.0 ± 1.88 |
| 2 | 900 | 10 | 3.95 ± 0.17 | 57.2 ± 2.46 |
| 3 | 1000 | 10 | 4.57 ± 0.11 | 66.2 ± 1.59 |
| 4 | 1100 | 10 | 4.19 ± 0.19 | 60.7 ± 2.75 |
| 5 | 1200 | 10 | 3.71 ± 0.09 | 53.8 ± 1.30 |

**Table 2**
Summary of Two-Step sintering conditions.

| Conditions | TEMP1 (°C) | Time1 (h) | TEMP2 (°C) | Time2 (h) |
|---|---|---|---|---|
| TSS1 | 1350 | 1 | 1213 | 10 |
| TSS1 | 1382 | 1 | 1213 | 10 |
| TSS1 | 1450 | 1 | 1213 | 10 |
| TSS2 | 1350 | 1 | 1213 | 20 |
| TSS2 | 1382 | 1 | 1213 | 20 |
| TSS3 | 1250 | 1 | 1100 | 20 |
| TSS3 | 1382 | 1 | 1100 | 20 |

microwave sintering, which may cause excessive grain growth due to liquid phase formation [1]. Chen and Wang [18] developed an effective approach, two-step sintering (TSS), for $Y_2O_3$ fabrication, which obtained fully dense nanoceramics by fine-tuning the "kinetic window" between grain boundary diffusion and grain boundary migration. However, $Gd_2Zr_2O_7$ ceramics fabricated with nanoparticles by pressureless sintering has not been previously reported.

Herein, we report a simple and cost-effective pressureless method containing a two-step temperature schedule to manufacture $Gd_2Zr_2O_7$ nanoceramics with high density. The ceramic samples were fully characterized. The fabrication process was analyzed and compared with the conventional, one-step sintering method. Specifically, we interpreted the conventional sintering process, in which the nanoceramics were sintered at various temperatures. The temperature effects on grain growth behaviors and densification mechanisms were analyzed and discussed. For the $Gd_2Zr_2O_7$ nanoceramics system, the size of nanoscale grains of starting powders plays an important role. On the other hand, in the two-step sintering, the sintering temperature in the first step follows the behavior of conventional sintering. Moreover, several different TSS programs were designed to study the effect of sintering temperature, holding time and the grain size of the starting powder on the formation of $Gd_2Zr_2O_7$ ceramics, especially, its relative density and the grain growth.

## 2. Experimental procedure

Solvothermal method was used in sample preparation. Specifically, the starting materials, $Gd(NO_3)_3{\cdot}6H_2O$ (>99.99%, Aladdin) and $ZrOCl_2{\cdot}8H_2O$ (>99.99%, Aladdin), were mixed according to the appropriate molar ratios of 1:1 and dissolved in deionized water with a concentration of 0.03 mol/L ($Gd^{3+}$ and $Zr^{4+}$). This mixture was pumped into diluted ammonium hydroxide until the pH reached 10.3. The gelling product was filtered and washed for two rounds, with deionized water (first round) and ethyl alcohol (second round). Then, this homogeneous mixture dissolved in ethanol was introduced into a stainless-steel autoclave and kept at 200 °C for 24 h. The precipitates (precursors) were washed with ethanol and dried for dehydration to obtain the final powders, which were further sieved and calcinated at 500 °C for 2 h to produce the starting $Gd_2Zr_2O_7$ powders. In addition, to investigate the grain growth and densification of nanoceramics as the crystal size of powders varies, we calcinated the starting $Gd_2Zr_2O_7$ powders at a series of temperature, ranging from 800 °C to 1200 °C.

The green pellets, 7 mm in diameter and 2–3 mm in thickness, were obtained by uniaxial pressing of the calcinated nanopowders with various particle sizes (see Table 1), which were heated to 1250 °C at 5 °C/min and sintered for 10 h to fabricate the $Gd_2Zr_2O_7$ ceramics. In the conventional pressureless sintering method, a series of sintering temperatures ranging from 1250 to 1500 °C (holding 1 h) were applied. On the other hand, to fabricate nanoceramics with higher density, a two-step sintering approach (TSS, see Table 2) was introduced in the present study. Typically, in the TSS method, each sample was heated to a high temperature ($T_1$) at 5 °C/min, held for 5 min to 1 h. Subsequently, it was cooled down to a lower temperature ($T_2$) at 8 °C/min dwelling for 10–20 h.

The green density and the final densities of the sintered compacts were determined by the Archimedes method with kerosene and deionized water as immersion medium respectively, using the value 6.90 g/cm$^3$ as the theoretical density for all the samples. The phases (crystal structures) of all samples were examined by powder X-ray diffraction (XRD, Model DX-2700, Dandong Fangyuan Instrument Co, Ltd, Liaoning, China). Transmission electron microscopy (TEM, Tecnai G2 F20 S-TWIN, FEI, Hillsboro, OR) images were collected to analyze the microstructure and morphology of all powder samples. The microstructure of ceramics was monitored and analyzed by scanning electron microscopy (SEM, Model S-4800, Hitachi, Japan). The mean particle size of calcinated powders and the average grain size of bulk ceramics were determined by XRD data using Scherrer equation and also directly measured from the SEM images. Prior to SEM experiments, the samples were polished and thermally etched in air for 2 h at a temperature 200 °C below the sintering temperature.

## 3. Results and discussion

### 3.1. Characteristics of powders

The microstructure of $Gd_2Zr_2O_7$ nanopowders is presented in Fig. 1. According to the TEM images, the starting powders calcined at 500 °C are composed of spherical particles with homogeneous size distribution. The mean particle size of the powder is 4 nm, which is consistent with the average grain size calculated from XRD data. The XRD patterns of the starting nanopowders calcinated at different temperatures, from 800 to 1200 °C (2 h) are shown in Fig. 2(a). All samples appear to be metastable fluorite phase. As calcination temperature increases clear diffraction peak narrowing is observed. This suggests that the grain size (crystallite growth) of nanopowders is a function of calcination temperature. The grain sizes can be derived quantitatively from the XRD data using Scherrer equation. Specifically, the grain sizes are confirmed to be nano-sized, ranging from 4 to 40 nm (see plot in Fig. 2(b)).

### 3.2. Conventional sintering

The relative density (%) and grain size (nm) of ceramics are plotted in Fig. 3 as a function of calcination temperature applied on the starting powders. Since all ceramics were sintered in air at 1250 °C with a soaking time about 10 h, the general trends of plot a and b in Fig. 3 reflect the effect of calcination temperature on relative density and grain size. Generally, higher temperature can provide sufficient driving force resulting in ceramics with higher density. At relatively low temperature, the relative density of sintered $Gd_2Zr_2O_7$ nanoceramics increases as the grain size of powders increases. Interestingly, the relative density reaches a maximum (80%) at about 1000 °C (see plot in Fig. 3). The corresponding ceramic microstructure of this maximum point is shown in Fig. 4(c). Further calcination temperature increase beyond 1000 °C leads to relative density of ceramics depression from 80 to 75%. In con-

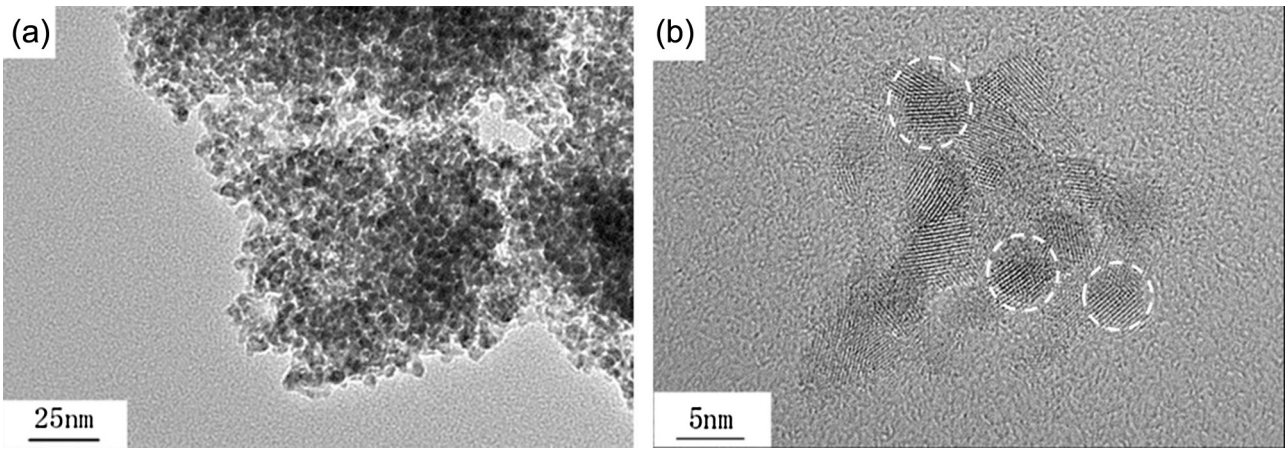


**Fig. 1.** The transmission electron microscopy (TEM) images of $Gd_2Zr_2O_7$ nanopowders.

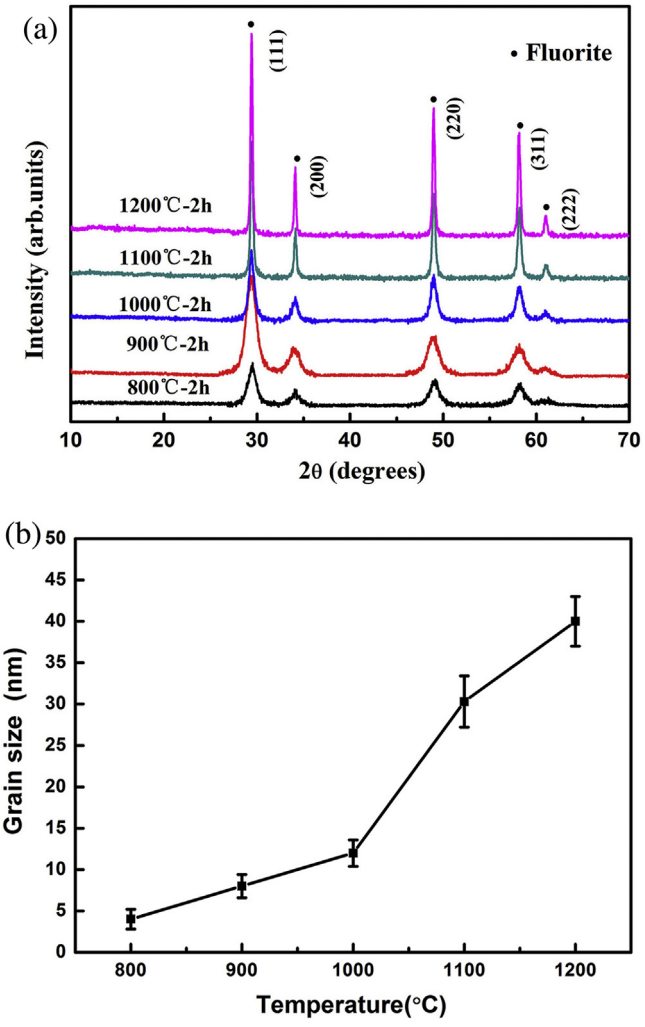


**Fig. 2.** XRD patterns (a) and grain sizes (b) for the $Gd_2Zr_2O_7$ powders synthesized at different temperatures for 2 h.

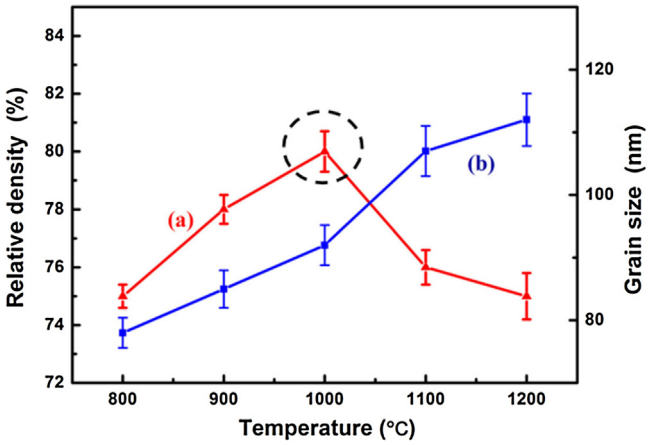


**Fig. 3.** Starting powders calcination temperature dependence of the relative density and grain size of $Gd_2Zr_2O_7$ ceramics sintered at 1250 °C for 10 h.

trast, the grain size of obtained ceramics derived from the SEM images using line intercept method (150 grains) exhibits to be a positive function of calcination temperature. Specifically, the grain size of ceramics increases from 78 nm (powders calcined at 800 °C) to 112 nm (powders calcined at1200 °C). At 1000 °C, the ceramics grain size is 90 nm. This set of data suggests that for the conventional pressureless sintering method the sample obtained from powders calcined at 1000 °C presents the optimized property, showing a relatively high density of 80% with grain size averaging 90 nm.

The SEM images are presented in Fig. 4 to elucidate the density and microstructure evolutions of $Gd_2Zr_2O_7$ ceramics sintered at 1250 °C. Interestingly, the ceramics fabricated from the powders calcinated at 1000 °C have the least number of pores (see Fig. 4(c)). Regardless crystallization acceleration, sintering of ceramics prepared using starting powders with smaller particle size leads to stronger driving force for densification (Fig. 4). In contrast, large size particles result in formation of relatively larger pores in the green compacts. These pores are more difficult to eliminate even using much higher sintering temperature and/or longer sintering time [19]. Further sintering introduces not only grain growth, but also formation of expended pores (see Fig. 4(c)–(e)). Indeed, pore coalescence due to grain arrangement is commonly observed in sintering studies [20]. Once the pores and particles are too large, low sintering temperature, such as 1250 °C, may not be sufficient enough to enable the rearrangement process. These results suggest that powders with distinct particle size and wide pore size distribution clearly lead to the densification variation of the final ceramic products. In other words, the densification of nanoceramic is tightly correlated to the particle and pore sizes of starting powders.

The $Gd_2Zr_2O_7$ nanoceramics prepared with powders calcinated at 1000 °C were sintered at various temperatures until the desired densification level was achieved. The grain growth rate of these

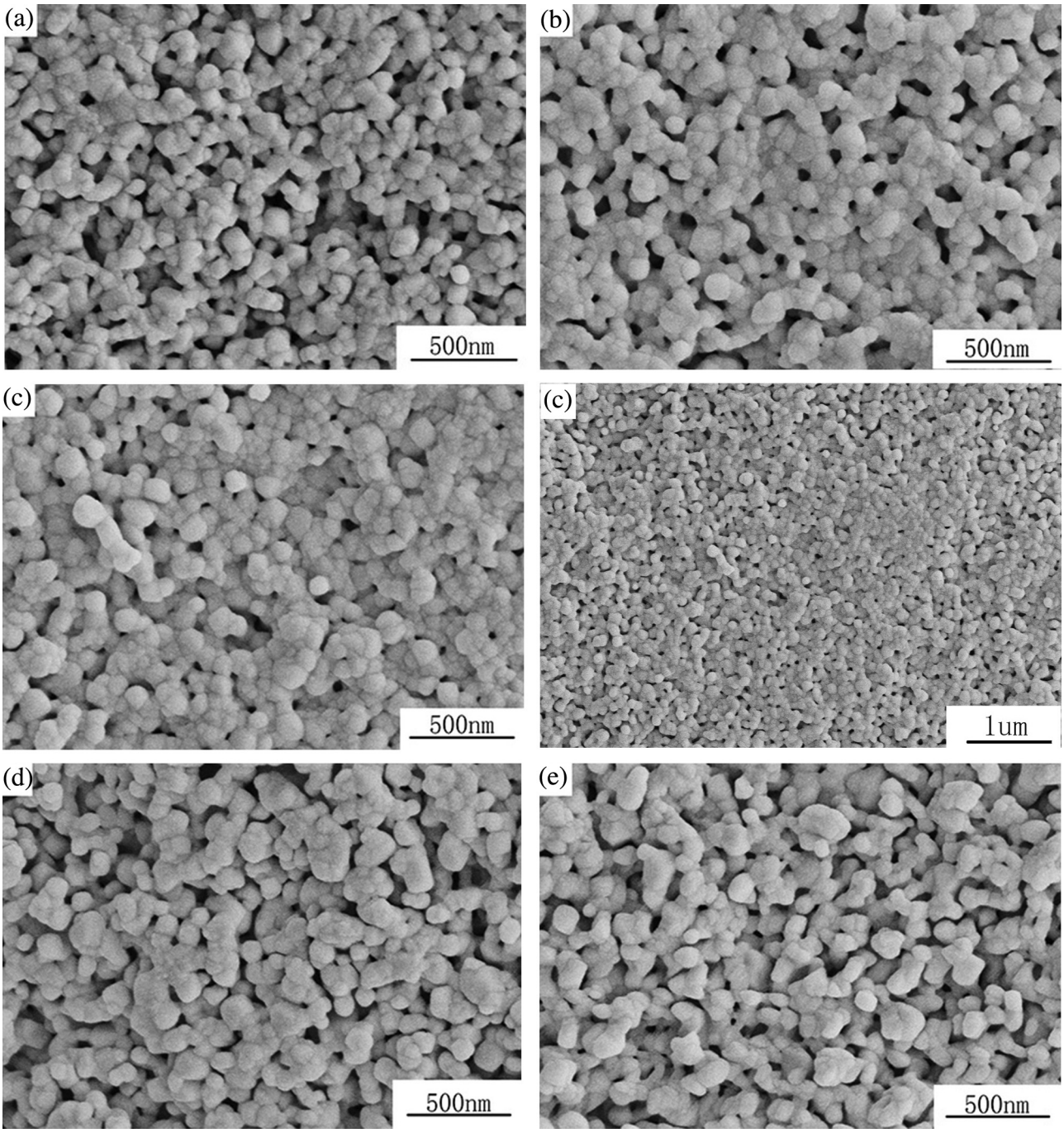


**Fig. 4.** Scanning electron microscopy (SEM) images of $Gd_2Zr_2O_7$ ceramics sintered at 1250 °C from powders calcinated at (a) 800, (b) 900, (c) 1000, (d) 1100, and (e) 1200 °C.

ceramics is plotted in Fig. 5(a). Rapid grain growth can be avoided at below 1400 °C. However, once sintered at 1450 °C, the sample grain size grows quickly to 160 nm. As temperature increases, the number of large grains increases accordingly [21]. On the other hand, the densification behavior of nanoceramics becomes increasingly significant as the sintering temperature increases (see Fig. 5(b)). Particularly, the increasing rate of relative density appears to be slower in low temperature sintering. Between 1300 and 1450 °C, a much more positive temperature rising rate is observed, which is in directly proportion to the sintering temperature. Further sintering at higher temperature results in decreased rate of densification. However, a higher relative density, around 90%, is confirmed when the temperature goes beyond 1450 °C. Interestingly, a previous report suggests that the open pores are typically observed during the intermediate stage of sintering, which corresponds to collapse and formation of closed pores [15]. When the relative density exceeds 90%, the closed porosity is filled by atomic diffusion. Moreover, fast grain coarsening is usually accompanied by grain boundary migration, which is owing to closed pore coalescence. In this work, we have successfully obtained $Gd_2Zr_2O_7$ nanoceramics with a relative density of 86% (1400 °C, 1 h holding time).

### 3.3. Two-step sintering

To achieve higher densification and finer grain size, we designed a two-step sintering method to prepare $Gd_2Zr_2O_7$ nanoceramics. Optimized grain size at nanoscale is critical towards successful fabrication of nanoceramics. Previous studies suggest that sample

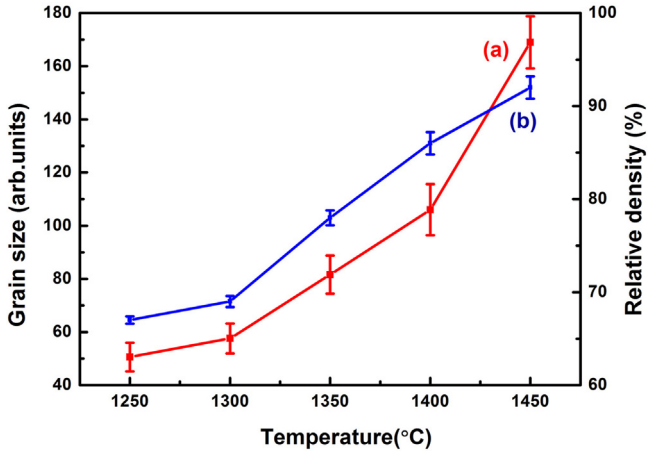


**Fig. 5.** a) Grain growth b) and relative density of the $Gd_2Zr_2O_7$ ceramics fabricated using conventional sintering method. Data were plotted as a function of sintering temperature (10 h).

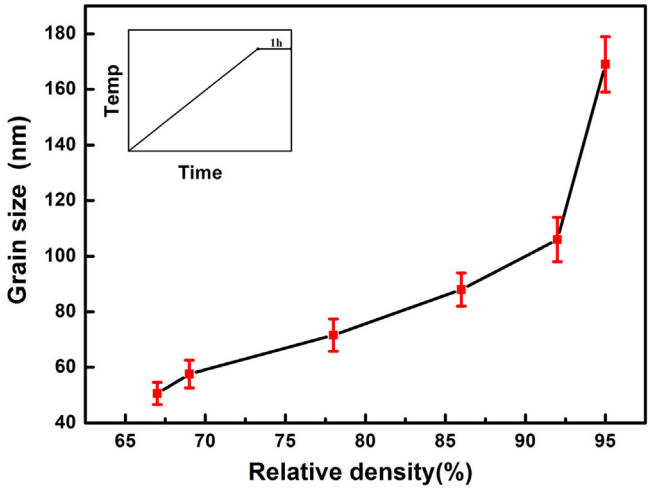


**Fig. 6.** Grain size of $Gd_2Zr_2O_7$ ceramics as a function of relative density (%) in conventional sintering for 1 h.

with relative density higher than 75% after the first-step sintering is necessary to achieve successful two-step sintering [10,11]. As a comparison, the $Gd_2Zr_2O_7$ ceramics were sintered in the first-step sintering at a temperature (T1) for 1 h followed by cooling down to room temperature. The average grain size of the ceramics evolves as a function of relative density during the conventional pressureless sintering (see Fig. 6). Increasing of relative density is usually accompanied by rapid grain growth in normal sintering [18]. When the temperature in the first-step sintering is less than 1400 °C, fast grain growth can be avoided (grain size between 78 and 90 nm). Further sintering leads to significant grain coarsening. In summary, the optimum sintering temperature scale for the first step of the two-step sintering is close to 1350 °C.

Fig. 7 shows the grain growth as a function of densification of $Gd_2Zr_2O_7$ ceramics sintered by the two-step method. The pore morphology achieved after the first step of treatment strongly suggests that low heating temperature is critical [4] since smaller grain size accelerates the speed of pore elimination. Compared with the conventional pressureless sintering demonstrated in Fig. 6, we successfully achieved $Gd_2Zr_2O_7$ nanoceramics with higher density and smaller grain size using the two-step sintering. For the nanoceramics sintered with powders calcinated at 1000 °C, the grain size of $Gd_2Zr_2O_7$ ceramics are very well-controlled, ranging from 80 to 90 nm. Heating beyond 1380 °C led to increasing of porosity in

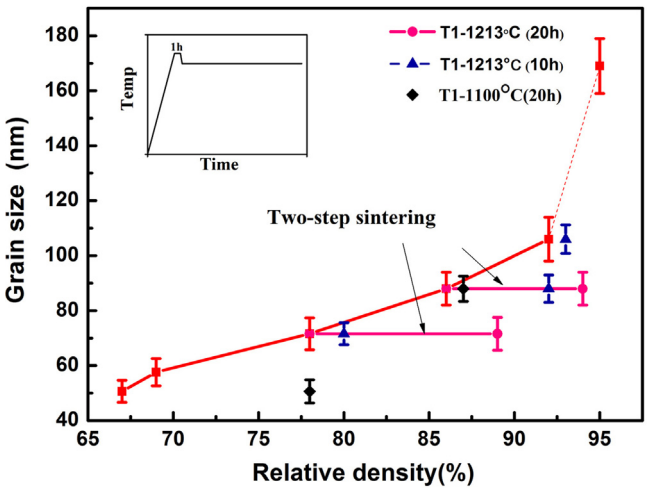


**Fig. 7.** Grain size of $Gd_2Zr_2O_7$ ceramics prepared via the two-step sintering approach as a function of relative density. The sample heating profile is shown in the figure inset. Three experimental conditions were applied to compare with the conventional sintering method.

ceramics, while below 1380 °C, much less number of pores was observed.

The SEM images of $Gd_2Zr_2O_7$ ceramics sintered in three distinct conditions are shown in Fig. 8. Specifically, closed pores distribute extensively between particles during the first sintering condition (TSS-1) with a holding time of 10 h in the second step (see Fig. 8a). The relative low degree of densification is largely due to insufficient time for grain diffusion. Pore structures observed in the second sintering condition (TSS-2, 1350 °C) are demonstrated in Fig. 8(b). Once the holding time in the second step is longer than 20 h, a nearly pore-free microstructure without abnormal grain growth is clearly detected (see Fig. 8(c)). In such sintering condition, the grain size of $Gd_2Zr_2O_7$ nanoceramics measured from the SEM image is around 83 nm, which is in excellent arrangement with the XRD results. Additionally, the sintered samples also present high relative density (93%). For the third sintering condition (TSS-3) (see Fig. 8(d)), we found that reducing temperature in the second step to 1100 °C has negative effect. Densification of ceramics using this approach (TSS-3) results in sample similar as that of conventional sintering.

Grain boundary migration is nearly always associated with grain growth, while the grain boundary diffusion usually leads to densification. This forms the basis for the two-step sintering method, with which we were able to fabricate dense ceramics with a fine grain size through fine-tuning the competing kinetics between grain-boundary diffusion and grain-boundary migration [10,11]. Our study clearly suggests that the second-step in two-step sintering can promote the densification and maintain the particle size without introducing detectable grain growth. In sharp contrast, increasing of relative density is almost always accompanied by rapid grain growth in the conventional sintering [22]. The low temperature in the second-step sintering may not be sufficient enough to provide higher activation energy for grain boundary migration, which may keep the grain-boundary diffusion active, yet may suppress grain boundary mobility. As the temperature increases, the inhibition of grain boundary motion decreases. The direct result is that grain coarsening is possible. Typically, migration of grain boundary happens upon reaching the highest surface energy [15], which occurs at the necks between grains first. Such thermodynamic and kinetic factors are very well manipulated to in our study on $Gd_2Zr_2O_7$ ceramics preparation. In summary, high density $Gd_2Zr_2O_7$ ceramics with fine grain size distribution has been successfully fabricated by two-step sintering.

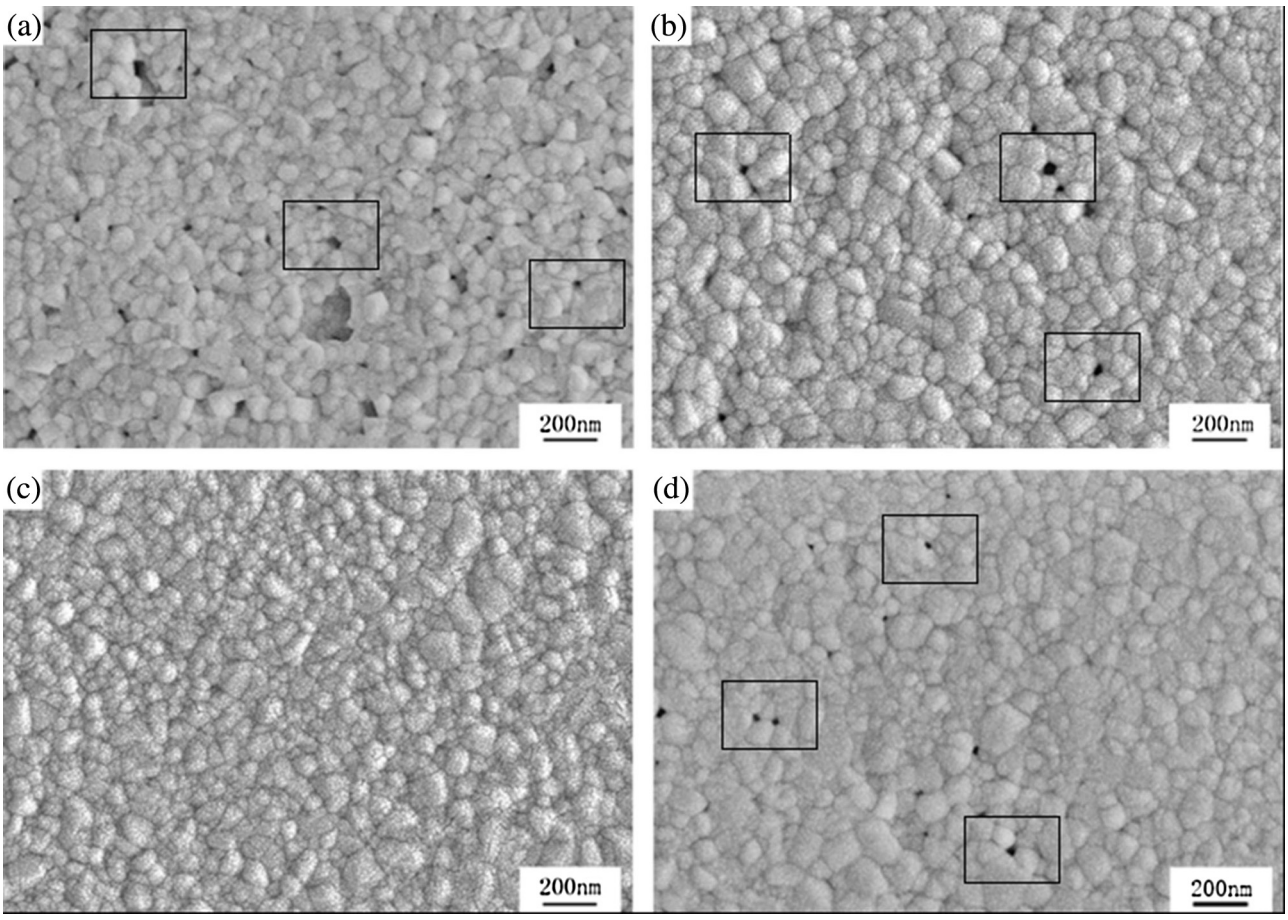


**Fig. 8.** Scanning electron microscopy (SEM) images of $Gd_2Zr_2O_7$ nanoceramics fabricated by the two-step sintering method. Sintering temperature profiles are (a) 1382 °C followed by 1213 °C for 10 h, (b) 1350 °C followed by 1213 °C for 20 h, (c) 1382 °C followed by 1213 °C for 20 h, (d)1382 °C followed by 1100 °C for 20 h.

## 4. Conclusions

High density $Gd_2Zr_2O_7$ ceramics with nanometer grain size was obtained by using a pressureless sintering method. The sample densification is tightly correlated to the particle size of the starting powders. This is originated from rearrangement of particles and pores in the green compacts. Meanwhile, as temperature increases, grain growth of $Gd_2Zr_2O_7$ nanoceramics was observed. The $Gd_2Zr_2O_7$ nanoceramics with relative density around 80% can be obtained by conventional sintering at 1250 °C. In contrast, for $Gd_2Zr_2O_7$ initially heated to 1382 °C, ceramics with higher density and closed packed configuration of nanoparticles was obtained after holding at 1213 °C for 20 h, which did not result in additional grain growth. Specifically, the $Gd_2Zr_2O_7$ nanoceramic fabricated using the pressureless two-step sintering method, has improved relative density (93%) as well as ultrafine grain size (83 nm). In addition, the grain-boundary diffusion was separated effectively from grain growth by controlling the temperature and soaking time in the first and second step of sintering. This two-step sintering method may provide an efficient yet economic pathway in nanostructured rare-earth zirconates fabrication, which can be applied as nuclear waste forms and thermal barrier coatings.

## Acknowledgements

This work was supported by the National Natural Science Foundation of the People's Republic of China under Grant Nos. 11505122 and 91326103, the CCS Project under Grant No. YK2015-0602004, and the Science and Technology Innovation Team of Sichuan Province under Grant No. 15CXTD0025. D. W. thanks the institutional funds from the Gene and Linda Voiland School of Chemical Engineering and Bioengineering at Washington State University.

## References

[1] K. Lu, Sintering of nanoceramics, Int. Mater. Rev. 53 (2008) 21–38.
[2] M. Cain, R. Morrell, Nanostructured ceramics: a review of their potential, Appl. Organomet. Chem. 15 (2001) 321–330.
[3] D. Shah, P. Maiti, E. Gunn, D.F. Schmidit, D.D. Jiang, C.A. Batt, Dramatic enhancements in toughness of polyvinylidene fluoride nanocomposites via nanoclay-directed crystal structure and morphology, Adv. Mater. 16 (2004) 1173–1177.
[4] K.N.P. Kumar, K. Keizer, A.J. Burggraaf, T. Okubo, H. Nagamoto, S. Morooka, Densification of nanostructured titania assisted by a phase-transformation, Nature 358 (1992) 48–51.
[5] Y.H. Zhen, J.F. Li, Normal sintering of (K,Na)$NbO_3$-based ceramics: influence of sintering temperature on densification, microstructure, and electrical properties, J. Am. Ceram. Soc. 89 (2006) 3669–3675.
[6] S.J. Dillon, M. Tang, W.C. Carter, M.P. Harmer, Complexion: a new concept for kinetic engineering in materials science, Acta Mater. 55 (2007) 6208–6218.
[7] T. Sano, G.S. Rohrer, Experimental evidence for the development of bimodal grain size distributions by the nucleation-limited coarsening mechanism, J. Am. Ceram. Soc. 90 (2007) 211–216.
[8] R.L. Coble, Sintering crystalline solids. 1. Intermediate and final state diffusion models, J. Appl. Phys. 32 (1961) 787–792.
[9] G. Suarez, Y. Sakka, T.S. Suzuki, T. Uchikoshi, X.W. Zhu, E.F. Aglietti, Effect of starting powders on the sintering of nanostructured $ZrO_2$ ceramics by colloidal processin, Sci. Technol. Adv. Mater. 10 (2009).
[10] C.L. Wan, Z.X. Qu, A.B. Du, W. Pan, Influence of B site substituent Ti on the structure and thermophysical properties of A(2)B(2)O(7)-type pyrochlore $Gd_2Zr_2O_7$, Acta Mater. 57 (2009) 4782–4789.
[11] Z.Y. Huang, J.Q. Qi, L. Zhou, Z. Feng, X.H. Yu, Y.C. Gong, M. Yang, Q.W. Shi, N. Wei, T.C. Lu, Fast crystallization of amorphous $Gd_2Zr_2O_7$ induced by thermally activated electron-beam irradiation, J. Appl. Phys. 118 (2015).

[12] Y. Zhang, L. Guo, X.X. Zhao, C.M. Wang, F.X. Ye, Toughening effect of $Yb_2O_3$ stabilized $ZrO_2$ doped in $Gd_2Zr_2O_7$ ceramic for thermal barrier coatings, Mater. Sci. Eng. A Struct. 648 (2005) 385–391.
[13] I.W. Chen, L.A. Xue, Development of superplastic structural ceramics, J. Am. Ceram. Soc. 73 (2009) 2585–2609.
[14] L. Ma, W.M. Ma, X.D. Sun, L.Y. Ji, J.A. Liu, K. Hang, Microstructures and mechanical properties of $Gd_2Zr_2O_7/ZrO_2$(3Y) ceramics, J. Alloy Compd. 644 (2015) 416–422.
[15] L. Ma, W.M. Ma, X.D. Sun, J.N. Liu, L.Y. Ji, H. Song, Structure properties and sintering densification of $Gd_2Zr_2O_7$ nanoparticles prepared via different acid combustion methods, J. Rare Earth 33 (2015) 195–201.
[16] Q. Xu, W. Pan, J.D. Wang, L.H. Qi, H.Z. Miao, K. Mori, T. Torigoe, Preparation and characterisation of $Gd_2Zr_2O_7$ ceramic by spark plasma sintering, Key Eng. Mater. 58 (2005) 1507–1510.
[17] X.R. Lu, Y. Ding, H. Dan, S.B. Yuan, X.L. Mao, L. Fan, Y.L. Wu, Rapid synthesis of single phase $Gd_2Zr_2O_7$ pyrochlore waste forms by microwave sintering, Ceram. Int. 40 (2014) 13191–13194.
[18] I.W. Chen, X.H. Wang, Sintering densele1 nanocrystalline ceramics without final-stage grain growth, Nature 404 (2000) 168–171.
[19] M.J. Mayo, D.C. Hague, D.J. Chen, Processing nanocrystalline ceramics for applications in superplasticity, Mater. Sci. Eng. A Struct. 166 (1993) 145–159.
[20] Y. Xiong, J.F. Hu, Z.J. Shen, V. Pouchly, K. Maca, Preparation of transparent nanoceramics by suppressing pore coalescence, J. Am. Ceram. Soc. 94 (2011) 4269–4273.
[21] S.H. Jung, S.J.L. Kang, Repetitive grain growth behavior with increasing temperature and grain boundary roughening in a model nickel system, Acta Mater. 69 (2014) 283–291.
[22] M. Mazaheri, A.M. Zahedi, S.K. Sadrnezhaad, Two-step sintering of nanocrystalline ZnO compacts: effect of temperature on densification and grain growth, J. Am. Ceram. Soc. 91 (2008) 56–63.